Bionatura
Latin American Journal of Biotechnology and Life Sciences

Article

Impacts of *Ganoderma lucidum* (Reishi mushroom) on the properties of electrospun polymeric nanofibers

Dalal Abbass Kadham[1,], Auda Jabbar Braihi[1,*], and Hanaa Jawad Kadham[1,*]*
[1] Polymer and Petrochemical Industries Department, College of Engineering Materials, University of Babylon, Iraq
**Correspondence: mat.hanua.jawad@uobabylon.edu.iq, Dalalabs035@gmail.com, Audajabbar@gmail.com*
Available from: http://dx.doi.org/10.21931/RB/CSS/2023.08.01.20

ABSTRACT

Three polymeric solutions, PVA, Collagen and Hyaluronic acid (HAc), were prepared and mixed by (55:22.5:22.5) ratios to prepare the net polymeric solution. Also, Ganoderma lucidum (G. lucidum) solution was prepared and added to the neat solution by three ratios (1wt%, 3wt% and 5wt%), which was then pumped by electrospinning technique to create a nanofiber bead. Solutions results showed that *G. lucidum* caused drag reduction, decreasing the viscosities, facilitating solution flow inside the needle and leading to the formation of fine nanofibers easily. Also, at low *G. lucidum* ratios, the electrostatic repulsion overcomes the surface tension, which enables fibers to escape from the "Taylor cone" tip and gather on the collector. As well as the electrical conductivity increased due to the ease of movement of HAc ions due to viscosity reduction. FTIR results proved no losses of any component of the net blend, and there is no chemical reaction among them. Results of the obtained nanofiber showed that, with the *G. lucidum* addition, there is an increment in fiber diameter, number of beads, the goodness of orientation and surface roughness. *G. lucidum* also reduced the wettability, the crystallinity and the enthalpy consumed during the thermal transition.

Keywords: Ganoderma lucidum, FESEM, Directionality Histogram, Electrospinning, Wettability

INTRODUCTION

Genus Ganoderma is found in the genus Ganoderma of the kingdom Fungi, the phylum Basidiomycota, the subphylum Agaricomycotina, the order Polyporales, and the family Ganodermataceae [1]. Ganoderma lucidum is an edible woody-brown saprotrophic fungus that lives on dead or dying trees and old stumps or logs. Also known as Reishi or Lingzi mushroom, it is very typical for traditional Chinese medicine[2].

Antitumor, immune modulation, liver protection, and other bioactivities can be found in *G. lucidum* spores [3].

This mushroom is commonly grown in Malaysia because of the country's year-round dampness and high temperatures. Polysaccharides and triterpenoids found in *G. lucidum* fruiting bodies may have therapeutic potential in treating or

preventing peripheral or central inflammatory disorders, according to a chemical study. Bioactive antioxidant metabolites can be found in a variety of Ganoderma species [4]. As a result of their minimal risk of side effects, mushrooms and other herbal medicines are increasingly being used as nutraceuticals, food supplements and cosmeceuticals.

Numerous *G. lucidum* triterpenes exhibit significant biological action Figure 1 against a wide range of diseases. Cancer [5], antioxidant [6], immunomodulator [7], anti-inflammatory, hypocholesterolemic [8], hypoglycaemic, antimicrobial [9], cardioprotective, antiarthritic, anti-hyperpigmentation, proapoptotic, antiandrogenic, anti-allergic and antinociceptive.

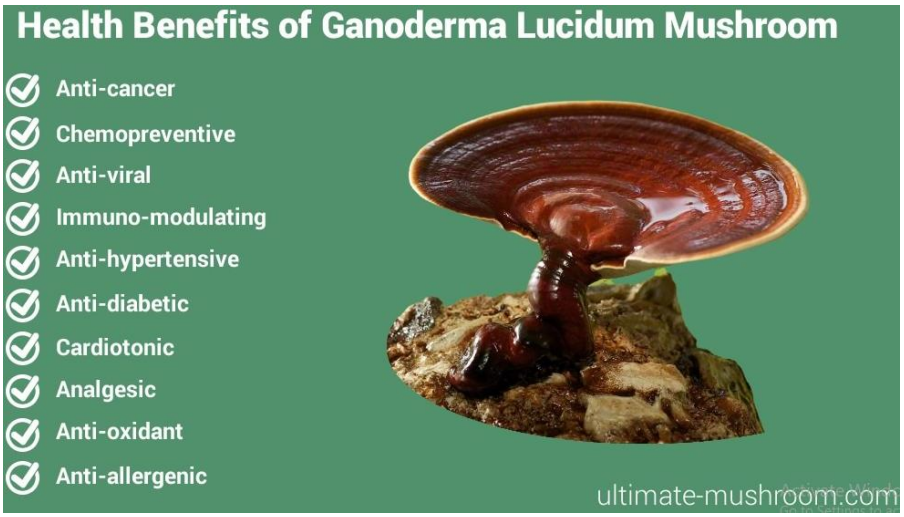

Figure 1. Benefits of Rishi Mushroom [10]

It is possible to dissolve PVA in water because it has several hydroxyl groups attached to the side chains. As a result of its high hydrophilicity, processability, and biocompatibility, as well as its remarkable chemical resistance and film-forming ability, it has received a great deal of attention[11]. Because of these characteristics, it is widely used in various industrial applications, including medical wrapping membranes [12], medication delivery, adhesives and thickeners, filtration, and gas barriers. Monofilaments of PVA were spun in the fiber industry to strengthen concrete. Electrostatic spinning has been used to produce ultrafine PVA fibers, which have recently been studied intensively for biomedical applications [13].

A polymer of the glycosaminoglycan family, hyaluronic acid (HA), is naturally found in the extracellular matrix (ECM) of tissues [14]. There are large concentrations of it in cockscomb, synovial fluid, the vitreous humor of the human eye, and the umbilical cord. The proliferation and migration of cells are made easier during wound healing when the area has a moisture balance [15].

Many tissues, such as skin, bones, tendons, ligaments, and other connective tissues, naturally contain collagen as part of their extracellular matrix (ECM). Two α1 chains and one α2 chain comprise the primary structural and functional protein of collagen type I. Polymers derived from natural sources are structured in a repeating motif that generates a coiled structure from the chains that make them up. The fibril's unique subunit complement determines the polymer's physical characteristics [16].

MATERIALS AND METHODS

Materials

Poly (vinyl alcohol) (PVA) was purchased from Verdean house, Daryaganj, New Delhi-110002 (India), with a degree of hydrolysis (86.0 -89.0 %) and molecular weight of 85,000 g / mole. Collagen powder is a biodegradable polymeric material with a molecular weight (360,000) from CDH (India). Hyaluronic acid sodium salt (HAC) (10000-20000 kDa) with a purity of 99.31% was purchased from SRL Pvt. Ltd., India. Distilled water, *G. lucidum* purchased from DXN PHARMACEUTICAL SDN BHD, ingredients of reishi mushroom powder (G. lucidum): mycelium and fruit body.

Preparation of electrospinning solutions

Three polymeric solutions were prepared. PVA solution was prepared by dissolving 10g PVA in 90 ml DW and mixing at RT for 60 min. Collagen (Coll.) solution was prepared by dissolving 7 g collagen in 93 ml DW with continuous mixing at RT for 30 min. Hyaluronic acid solution (HAc) was prepared by dissolving 5.5 g HAc in 94.5 DW and mixing for 30 min. at RT.

(55:22.5:22.5) ratios mixed these three polymeric solutions for 60 min. Prepare the net polymeric solution (Solution A) at RT, which is then pumped by an electrospinning technique to create a nanofiber bead.

G. lucidum solution was prepared by dissolving 5 g of *G. lucidum* powder in 95 ml DW at RT for 10 h. This solution was added to the previous triple polymeric solution by three ratios (1wt%, 3wt%, and 5wt%), mixed carefully, injected into a syringe and pumped. The symbols B, C and D were adopted for these new solutions.

The electrospinning conditions were 1 ml/h flow rate, 19 KV voltage, and 20 cm distance between the needle and the flat aluminum foil-wrapped collector, which rotated at 600 rpm. It is worth noting that each of the four solutions was also pumped separately to evaluate their rheological properties.

Test

The viscosity test was done using “Brookfield DV-III Ultra Rheometer. The surface tension of the solutions was measured with a SL 200C - Optical Dynamic I Static Interfacial Tensiometer. Electrical conductivity test using an electrical conductivity device (model HANNA instruments - EC 214 conductivity Meter. FTIR test was carried out using (IRAFFINITY-1) (Shimatzu) to check the nanofiber structure. The morphology of the nanofibers was evaluated using field-emission scanning electron microscopy (FE-SEM) (MIRA3 TESCAN- FRANCE). The wettability test is achieved by Contact Angle Meter, manufactured in KINO Industry Co., Ltd., USA, with a contact angle range from 0° to 180°. DSC technique used to follow the thermal with 10˚C / min heating rate, 50- 400 ˚C span temperature using argon gas.

RESULTS

Solutions Results

Figure 2 shows the effects of *G. lucidum* addition on the viscosity-shear rate relationships for the prepared solutions. The viscosity of the neat solution (free from G. lucidum) is always higher than solutions containing G. lucidum. As well as the viscosity increased as *G. lucidum* increased but did not reach the viscosity of the neat solution

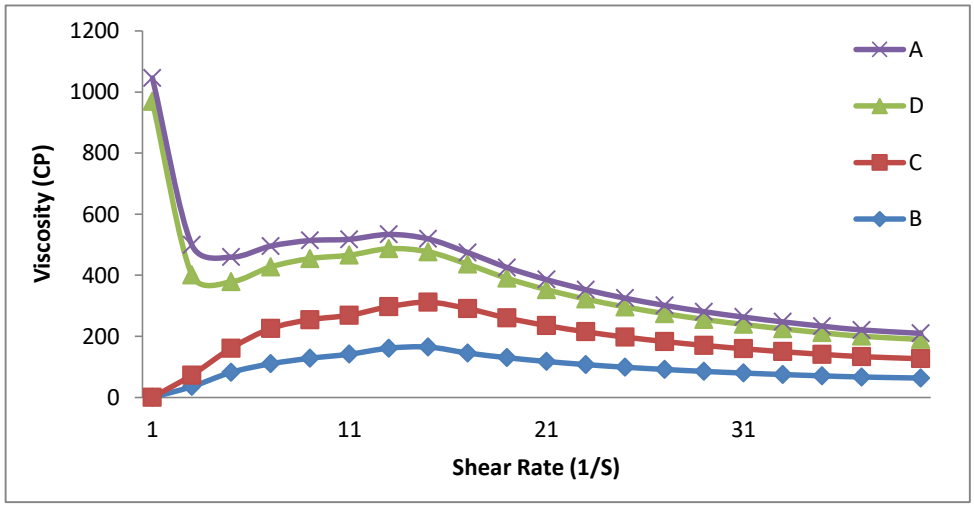

Figure 2. Relationship between viscosity and shear rate.

The *G. lucidum* content increased with surface tension to the extent that it exceeded the value of the neat blend at a higher *G. lucidum* ratio. At lower ratios (0.1 - 0.3 wt%), the surface tension decreased, which enabled the electrostatic repulsion to overcome the surface tension. This will enable the polymeric solution to escape from the "Taylor cone" tip and fly rapidly toward the collector.

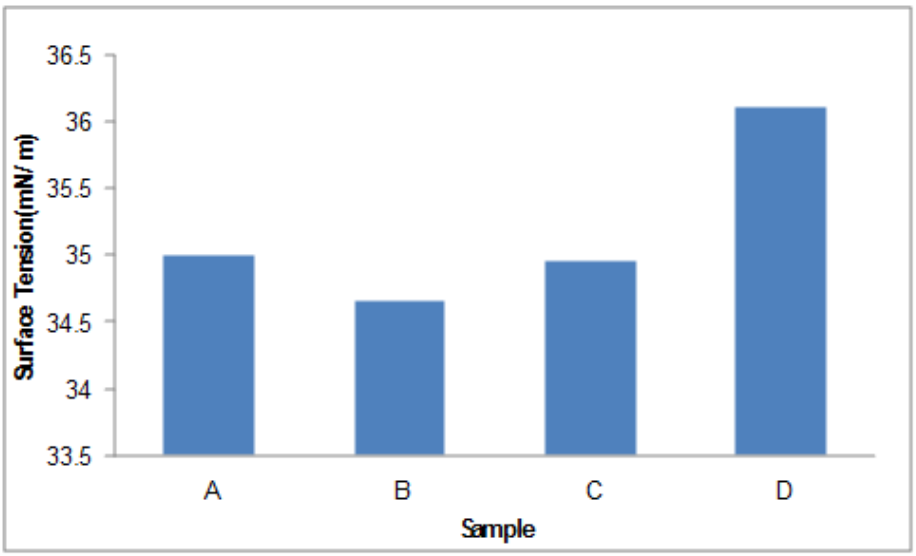

Figure 3. Surface tension for (A) net blend (B) blend with l wt.% *G. lucidum* (C) blend with 3 wt.% *G. lucidum* (D) blend with 5 wt.% *G. lucidum.*

FTIR Results

Figure 5 shows the FTIR spectrum of Collagen material, where the principal characteristics bands for Amide A, Amide I, Amide II and Amide III exist. The strong band around 3425.58 cm^{-1} belongs to the N=H stretching vibration mode.

The band at 2970 cm^{-1} refers to the asymmetrical vibration of the CH_2 group. The carbonyl group (C=O) stretching vibration for Amide I appears at 1651.07 cm^{-1}. At the position 1543.05 cm^{-1}, the Amide II appears through the in-plane bending of the N-H group. The in-plane deformations of both CH_2 and CH_3 groups appear at 1458.18 cm^{-1} and 1410.18 cm^{-1}, respectively. The in-plane deformation vibration mode of N-H appears at 1242.16 cm^{-1}, which confirms the Amide III Collagen type.

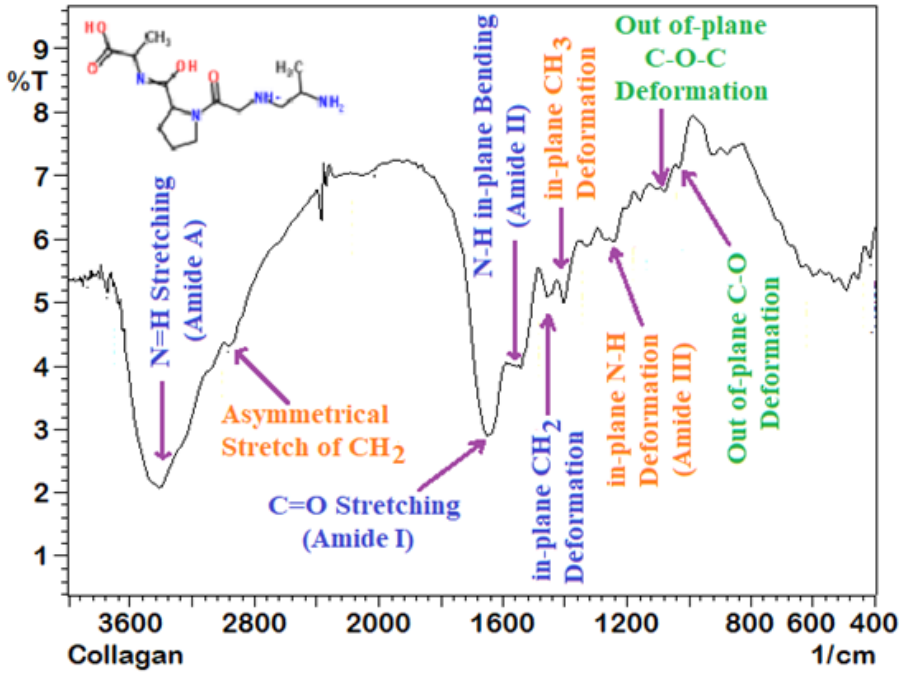

Figure 5. FTIR spectrum of collagen

Figure 6 shows the FTIR spectrum of the PVA polymer. The broad band around 3402.43 cm^{-1} is due to the stretching vibration of a hydroxyl group (-OH), while the band at 2939.52 cm^{-1} belongs to the stretching of the C–H alkyl group. The band at 1728.22 cm^{-1} indicates the incompletely hydrolyzed acetate to polyvinyl alcohol (PVA). The band at 1651.07 cm^{-1} belongs to the C=C stretching. The peak corresponding to the C-O stretching occurs at 1095.57 cm^{-1}

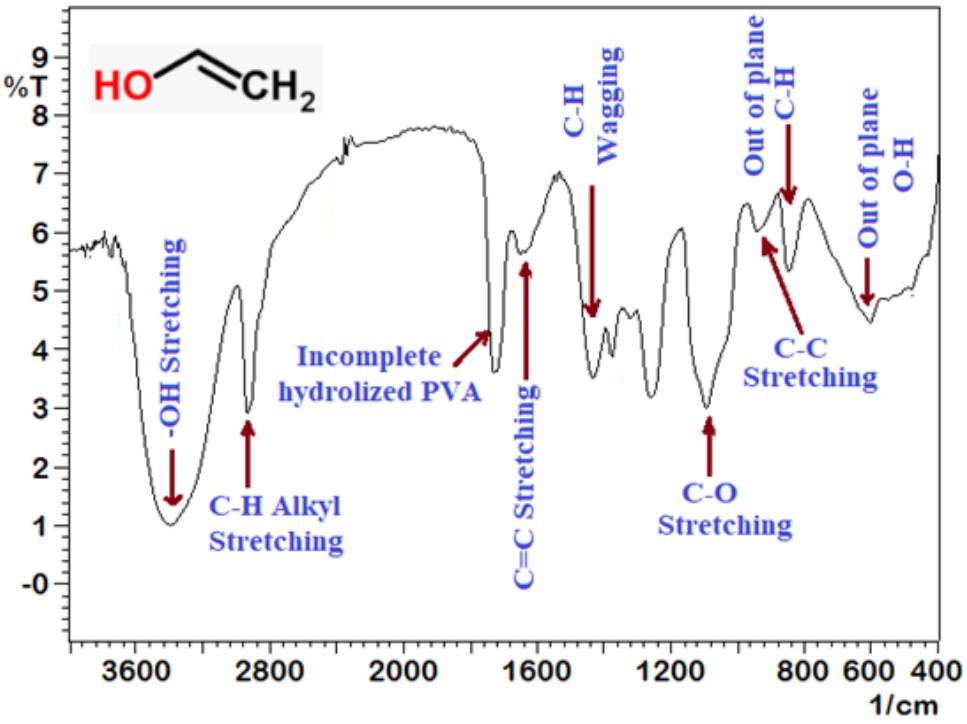

Figure 6. FTIR spectrum of PVA

The FTIR spectrum of hyaluronic acid (HAc) is shown in Figure 7. The broad-band from 3000 to 3700 cm^{-1} belongs to the combination of the O-H and N-H stretching. The band at 2931.80 cm^{-1} refers to the stretching vibration of the CH_2 group. The peak at 1620.21 cm^{-1} refers to the secondary Amide group (C=O group).

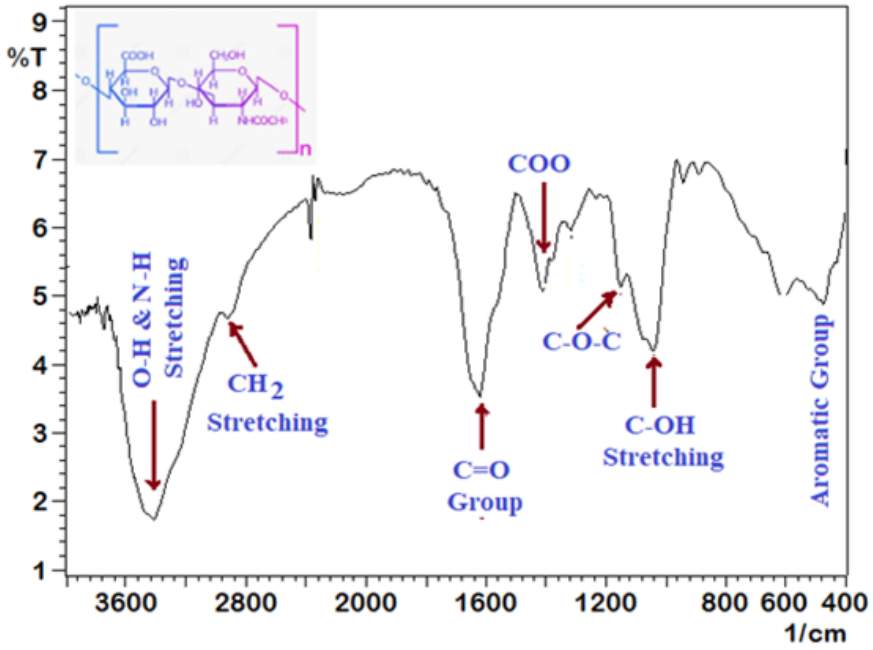

Figure 7. FTIR spectrum of Hac

Figure 8 shows the FTIR spectrum of the polymeric blend made from PVA, HAc and Collagen.

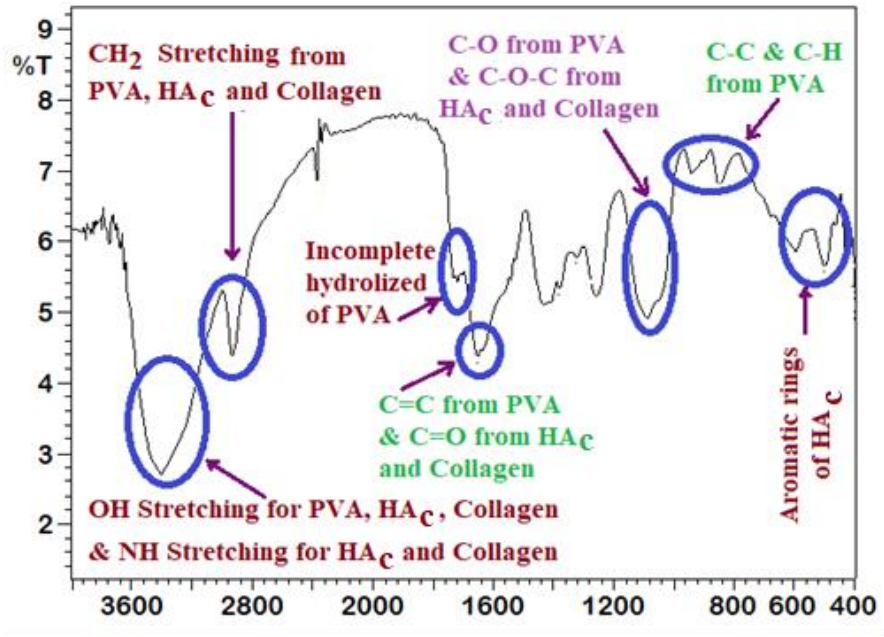

Figure 8. FTIR spectrum of the net polymeric blend

Wettability results

Adding 5 wt% *G. lucidum* Figure 9 increased the contact angle from 31℃ to 43.84º. This result coincides with the increment in surface tension.

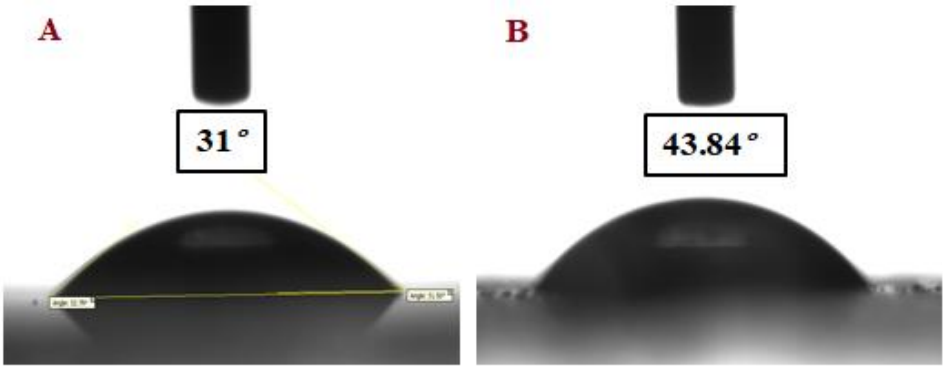

Figure 9. Contact angles for (A) neat blend nanofiber and (B) blend with 5 wt.% *G. lucidum*

Fesem Images

Figures 10 and 11 show the FESEM images and the diameter distribution of the resulting fibers, respectively. It is clear that as *G. lucidum* content increased, the fiber diameter and the number of beads increased. Compared with the morphology of the neat blend, the porosity increased linearly with *G. lucidum* and more branched fibers formed.

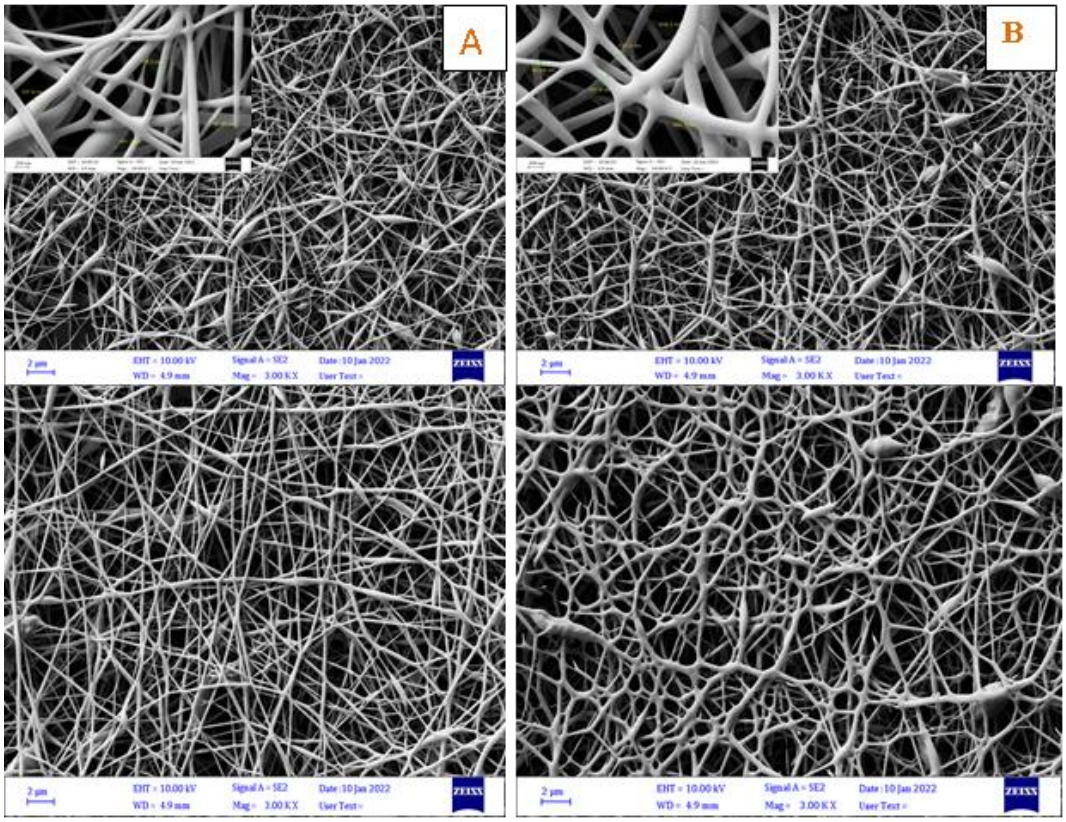

Figure 10. FESEM images for (A) neat blend nanofiber (B) blend with l wt.% *G. lucidum* (C) blend with 3 wt.% *G. lucidum* (D) blend with 5 wt.% *G. lucidum*

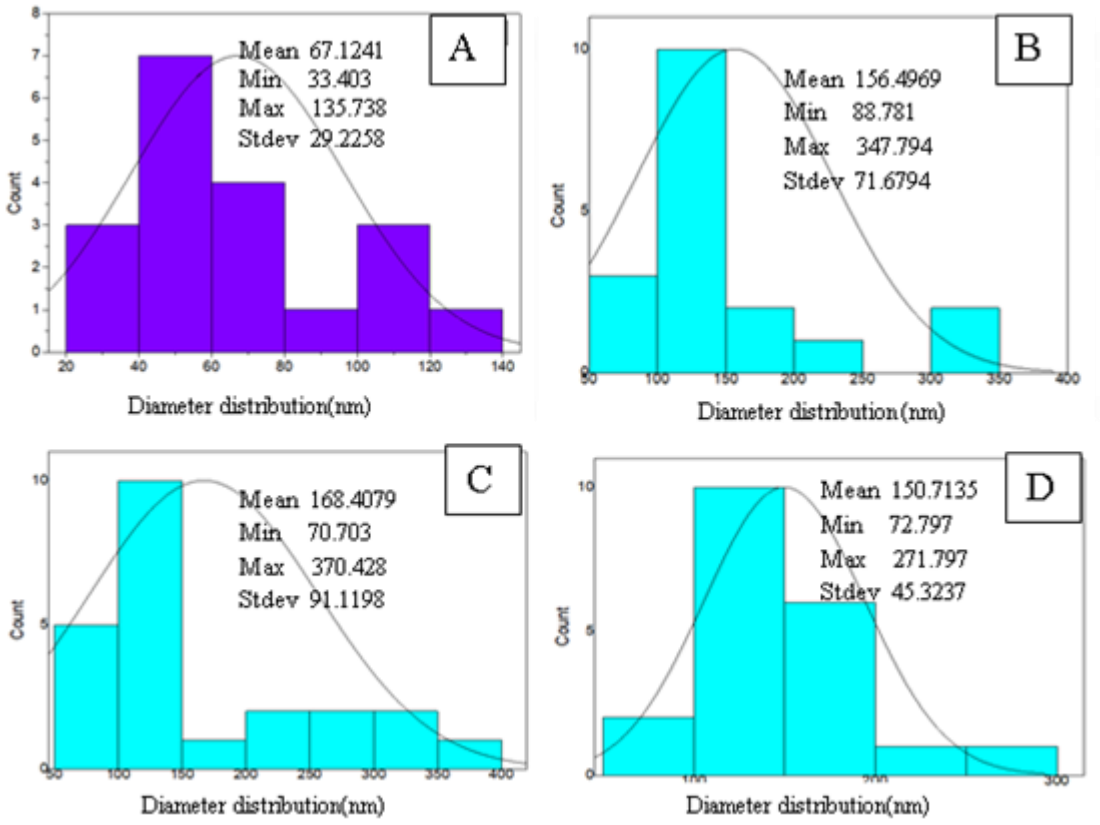

Figure 11. Diameter distribution of nanofiber (A) neat blend nanofiber (B) blend with l wt.% *G. lucidum* (C) blend with 3 wt.% *G. lucidum* (D) blend with 5 wt.% *G. lucidum*

Directionality analysis

Orientation parameters of the obtained nanofibers (Figure 12 and Table 1) were extracted from FESEM images using the Fiji Software.

Upon the *G. lucidum* addition, the preferred direction of the oriented nanofibers shifted from 48.36 to 53.84, as shown with the Gaussian profile. This profile showed that, in both cases, the fibers are oriented in random directions.

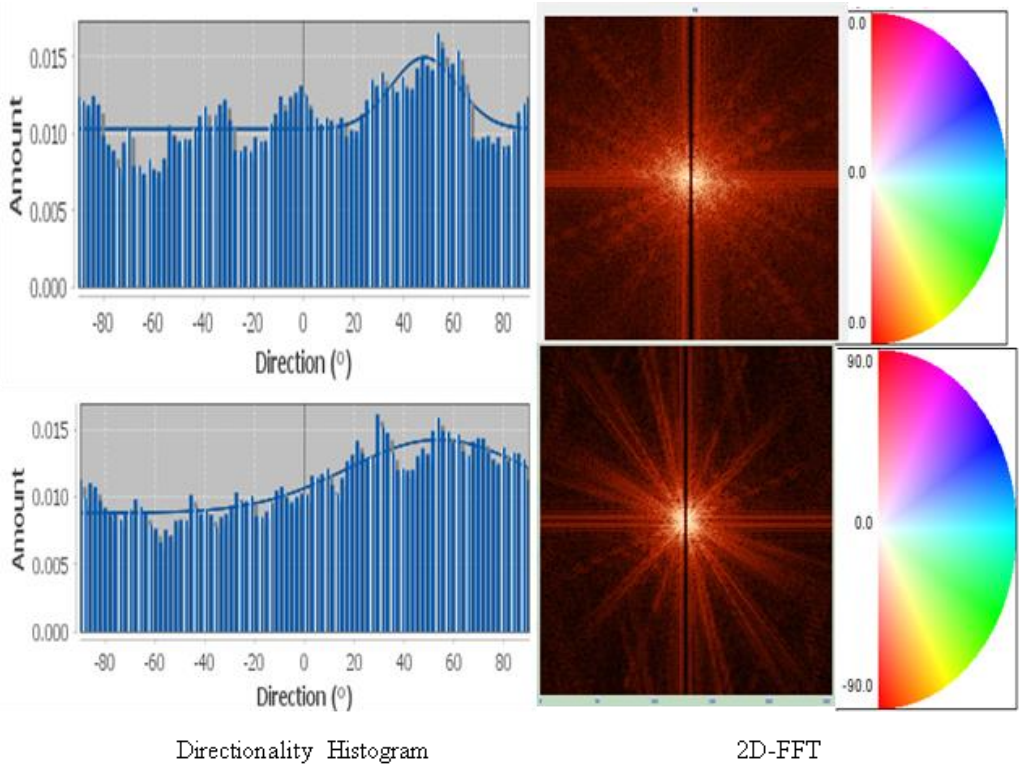

Figure 12. Directionality Histogram and 2D-FFT. For (A) neat blend nanofiber (B) blend with 5 wt.% *G. lucidum*

Nanofibers Sample	Direction (°)	Dispersion (°)	Amount	Goodness
Neat blend	48.36	0.34	0.34	0.49
Blend with 5 wt.% G. lucidum	53.84	36.61	0.69	0.80

Table 1. Directionality analysis for (A) neat blend nanofiber (B) blends with 5 wt.% G. lucidum

Differential Scanning Calorimetric (DSC)

DSC results (Figure 13) showed that compared to the single thermal transition for the neat blend, two transitions occurred upon *G. lucidum* addition. These two adjacent transitions happened on a wider temperature range and consumed lower enthalpy. For neat blend, the transition occurred from 79.110C to about 110 0C and needs 1065 J/g, while the *G. lucidum* addition facilitates the transition to occur at a relatively lower temperature (75.640C) and extends to about 1370C and needs a total enthalpy of 241.71 J/g. This is because the *G. lucidum* addition caused phase separation, which reflected, as seen earlier, in

increasing the porosity among fibers, reducing the crystallinity. As the porosity increases, the heat required for transition is less.

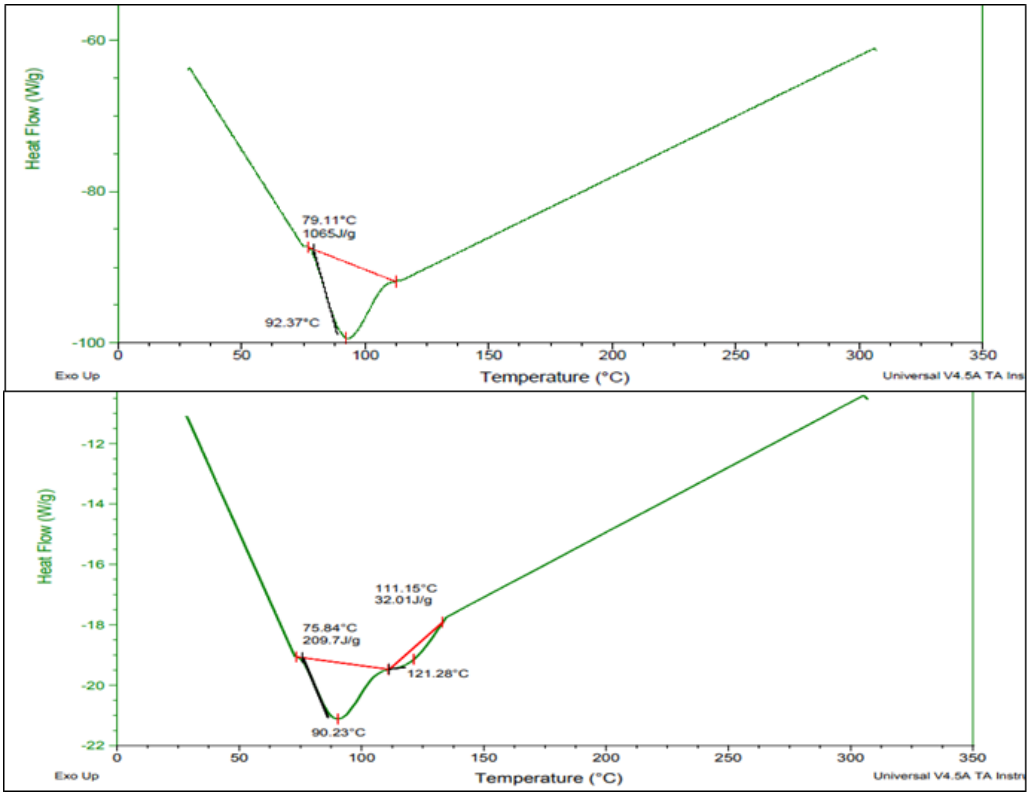

Figure 13. DSC thermographs of nanofiber for (A) neat blend (B) blend with 5 wt.% *G. lucidum*

Atomic force microscopy (AFM) results

Figure 14 and Table 2 monitored the surface roughness of the prepared fibers.

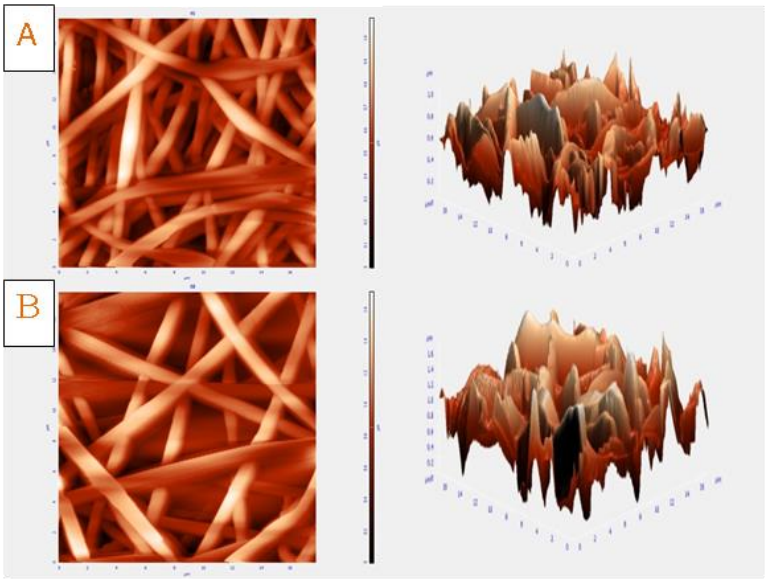

Figure 14. 2D and 3D- micrographs AFM images for (A) neat blend nanofiber (B) blend with 5 wt.% G. lucidum

The 2D and 3D AFM images provided evidence of increased porosity and fiber diameter upon *G. lucidum* addition. This addition also increased the surface roughness of the layer of the electrospun fibers, as evidenced by all the roughness parameters in Table 1. For example, the average roughness increased by 63.7%, the root mean square by 57% and so on.

Roughness parameter	Neat blend	Blend with 5 wt.% G. lucidum	Property Change (%)
Average Roughness, S_a (nm)	145.019	237.391	+ 63.7
Root Mean Square, S_q (nm)	183.626	288.307	+ 57
Peak-to-peak, S_y (nm)	1083.48	1705.61	+ 57.4
Ten-point height, S_z (nm)	543.762	850.484	+ 56.4
Surface skewness, S_{sk}	0.00383049	0.260757	+ 6707.4

Table 2. Roughness parameters of (A) neat blend nanofiber (B) blend with 5 wt.% G. lucidum

DISCUSSION

The solution result showed that *G. lucidum* generally caused drag reduction, which facilitates the flow of the new solutions due to the reduction in the friction forces among solution layers. This new pattern encourages fluid flow inside the needle, leading to the formation of fine nanofibers easily by the electrospinning technique.

Maximum viscosity is obtained at about 15 (s-1) shear rate and decreased for all solutions. This means that the forces among fluid layers will destroy beyond this shear rate, making these layers slip easily over each other. With surface tension, the same behavior (as viscosity behavior) occurs.

For the FTIR result, The presence of the carbohydrate moieties was confirmed by the appearance of pulses at 1080.14 cm-1 and 1033.85 cm-1, which refer to the out-of-plane deformations of CH2-O-CH2 and C-O, respectively. These results coincide with [17,18,19].

The peak corresponding to the C-O stretching occurs at 1095.57 cm−1. The out-of-plane vibrations of O-H and C-H groups occur at 601.79 cm-1 and 848.68 cm-1, respectively [20].

The band at 1411.89 cm-1 corresponds to the C-OO group in combination with the C=O group. The band at 1147.57 cm-1 belongs to C-O-C. The C-OH stretching occurs at 1041.56 cm-1[21]

All the pulses in the blend spectra are present in one or more of the three blend components, which means two things:

All three components (PVA, HAc and Collagen) are present in the blend, and there is no loss. There is no chemical reaction between the three components, and there is only physical interaction between the polymeric chains of the three components.

The pulses belong to the chemical structure of PVA (-OH, CH2, C=C, C-C, incomplete hydrolyzes of acetate and C-H) and are present in the blend spectrum with slight shifting. The same thing happened with the functional groups of HA (-OH, -NH, C=O and the aromatic rings) and Collagen (-OH, -

NH, CH2, C=C and C-O-C). This random orientation of most fibers can be attributed to repulsion forces during their movement towards the collector and to the atmosphere formed around the cylindrical collector, which rotates with it at high rotation speed (3500 rpm). This causes movement disturbances and forces the fibers to deviate from their path that is not perpendicular to the collecting axis. Also, there is an increment in the goodness of orientation nanofibers, as for FESEM Images. The mean diameter increased with *G. lucidum* addition from 67.1241.nm to reach its maximum value (168.4079) at 3 wt% addition. This result coincides with big beads and fused fibers forming at 5 wt% addition, as shown in Figure 9-D.

CONCLUSION

In this study, *G. lucidum* caused drag reduction, decreasing the viscosities, facilitating solution flow inside the needle and leading to the formation of fine nanofibers easily. Also, at low *G. lucidum* ratios, the electrostatic repulsion overcomes the surface tension, and the electrical conductivity increases due to the ease of movement of HAc ions due to viscosity reduction. FTIR results proved no losses of any component of the net blend, and there is no chemical reaction among them. The obtained nanofiber showed that, with the *G. lucidum* addition, there is an increment in fiber diameter, number of beads, the goodness of orientation and surface roughness. *G. lucidum* also reduced the wettability, the crystallinity and the enthalpy consumed during the thermal transition.

References

1. Zhou X, Lin J, Yin Y, Zhao J, Sun X, Tang K. Ganodermataceaenatural products and their related pharmacological functions. *The American Journal of Chinese Medicine*. **2007**; *35*:559–574.
2. https://ultimate-mushroom.com/edible/12-ganoderma-lucidum.html
3. Xin Wanga, Xianliang Chena, Zeming Qic, Xingcun Liub, Weizu Li, Shengyi Wang"A study of Ganoderma lucidum spores by FTIR microspectroscopy" Spectrochimica Acta Part A 91, **2012**, 285–289
4. Poh-Guat Cheng, Chia-Wei Phan, Vikineswary Sabaratnam, Noorlidah Ab+-dullah, Mahmood Ameen Abdulla, and Umah Rani Kuppusamy" Polysaccharides-Rich Extract of Ganoderma lucidum (M.A. Curtis:Fr.) P. Karst Accelerates Wound Healing in Streptozotocin-Induced Diabetic Rats" Evidence-Based Complementary and Alternative Medicine Volume, **2013**, PP:1-9,2013
5. M.F. Ahmad Ganoderma lucidum: *A rational pharmacological approach to surmount cancer J. Ethnopharmacol*. **2020**.
6. Yi Zhang, H. Cai, Z. Tao, C. Yuan, Z. Jiang, J. Liu, H. Kurihara, W. Xu ,Ganoderma lucidum spore oil (GLSO), a novel antioxidant, extends the average life span in Drosophila melanogaster. Food Sci. HumWellness. **2020**.
7. F. Ahmad, F.A. Ahmad, M.I. Khan, A.A. Alsayegh, S. Wahab, M.I. Alam, F. Ahmed ,Ganoderma lucidum: A potential source to surmount viral infections through β-glucans immunomodulatory and triterpenoids antiviral properties, *Int. J. Biol. Macromol*. **2021**, 10.1016/j.ijbiomac.06.122
8. M.A. Rahman, S. Hossain, N. Abdullah, N. Aminudin,Ganoderma lucidum Ameliorates Spatial Memory and Memory-Related Protein Markers in Hypercholesterolemic and Alzheimer's Disease Model Rats. Arch. NeurolNeurol. Disord. **2020**, p. 3
9. S. Savin, O. Craciunescu, A. Oancea, D. Ilie, T. Ciucan, L.S. Antohi, A. Toma, A. Nicolescu, C. Delea nu, F. Oancea,Antioxidant, Cytotoxic and Antimicrobial Activity of Chitosan Preparations Extracted from Ganoderma Lucidum Mushroom. Chem. Biodivers,17 ,**2020.**
10. https://ultimate-mushroom.com/edible/12-ganoderma lucidum.html, **2022.**
11. (Polyvinyl Alcohol-Iodine) Bio-Composites and Their Applications" *Eijppr*, **2017**, *7(5)*: PP: 1-8.

12. Auda J. Braihi, Jaleel K.Ahmed, Dalal A. Kadham" Preparing Medical (Polyvinyl-Iodine) As A Pressure Sensor and Investigation Its Physical Properties" *EIJPPR* ,**2017**, *7(1)*:34-41.
13. Syang-Peng Rwei and Cheng-Chiang Huang "Electrospinning PVA Solution-Rheology and Morphology Analyses" *Fibers and Polymers*. **2012**, *13(1)*: 44-50
14. J. Necas, L. Bartosikova, P. Brauner, J. Kolář, Hyaluronic acid (Hyaluronan): A review, Veterinarni Medicina. 53, **2008**. 397-411.
15. G. Kogan, L. Šoltés, R. Stern, P. Gemeiner, Hyaluronic acid: A natural biopolymer with a broad range of biomedical and industrial applications, Biotechnol. Lett. 29, **2007**; 17–256.
16. Sena Su , Tuba Bedir, Cevriye Kalkandelen ,Ahmet Ozan Başar Hilal TurkoğluŞaşmazel , Cem Bulent Ustundag, Mustafa Sengor, Oguzhan Gunduz" Coaxial and Emulsion Electrospinning of Extracted Hyaluronic Acid and Keratin Based Nanofibers for Wound Healing Applications" *European Polymer Journal*, **2021**; *142*.
17. Nancy P. Camacho,1 Paul West,1 Peter A. Torzilli,1 Richard Mendelsohn" FTIR Microscopic Imaging of Collagen and Proteoglycan in Bovine Cartilage" *Biopolymers Biospectroscopy*, **2001**; *62*, 1–8.
18. Karima Belbachir, Razia Noreen, Gilles Gouspillou, and Cyril Petibois" Collagen types analysis and differentiation by FTIR spectroscopy" Springer-Verlag, **2009**.
19. Tehseen Riaz, Rabia Zeeshan, Faiza Zarif, Kanwal Ilyas, Nawshad Muhammad, Sher Zaman Safi, Abdur Rahim, Syed A. A. Rizvib, and Ihtesham Ur Rehman" FTIR analysis of natural and synthetic collagen" Applied Spectroscopy Reviews, 53:9, 703-746
20. P.K. Khanna∗, Narendra Singh, Shobhit Charan, V.V.V.S. Subbarao, R. Gokhale, U.P. Mulik" Synthesis and characterization of Ag/PVA nanocomposite by chemical reduction method" Materials Chemistry and Physics 93, **2005**; 117–121
21. Hongyue Chen, Jing Qin and Yi Hu. Efficient Degradation of High-Molecular-Weight Hyaluronic Acid by a Combination of Ultrasound, Hydrogen Peroxide, and Copper Ion. *Molecules journal*. **2019**;*24(3)* , 617 .

Received: May 15, 2023/ Accepted: June 10, 2023 / Published: June 15, 2023

Citation: Kadham, D.A.; Braihi, A.J.; Kadham, H.J. Impacts of *Ganoderma lucidum* (Reishi mushroom) on the properties of electrospun polymeric nanofibers. Revis Bionatura 2023;8 (1) 20. http://dx.doi.org/10.21931/RB/CSS/2023.08.01.20